An Alamethicin Channel in a Lipid Bilayer: Molecular Dynamics Simulations

D. Peter Tieleman,* Herman J. C. Berendsen,* and Mark S. P. Sansom#
*BIOSON Research Institute and Department of Biophysical Chemistry, University of Groningen, 9747 AG Groningen, The Netherlands, and #Laboratory of Molecular Biophysics, Department of Biochemistry, University of Oxford, Oxford OX1 3QU, England

ABSTRACT We present the results of 2-ns molecular dynamics (MD) simulations of a hexameric bundle of Alm helices in a 1-palmitoyl-2-oleoylphosphatidylcholine bilayer. These simulations explore the dynamic properties of a model of a helix bundle channel in a complete phospholipid bilayer in an aqueous environment. We explore the stability and conformational dynamics of the bundle in a phospholipid bilayer. We also investigate the effect on bundle stability of the ionization state of the ring of Glu^{18} side chains. If all of the Glu^{18} side chains are ionised, the bundle is unstable; if none of the Glu^{18} side chains are ionized, the bundle is stable. pK_A calculations suggest that either zero or one ionized Glu^{18} is present at neutral pH, correlating with the stable form of the helix bundle. The structural and dynamic properties of water in this model channel were examined. As in earlier in vacuo simulations (Breed et al., 1996. *Biophys. J.* 70:1643–1661), the dipole moments of water molecules within the pore were aligned antiparallel to the helix dipoles. This contributes to the stability of the helix bundle.

INTRODUCTION

Channels formed by integral membrane proteins enable ions to move passively across lipid bilayers. They are important in numerous cellular processes, ranging from electrical signaling (Hille, 1992) to facilitating the uncoating of viral genomes (Sansom et al., 1998b). They form transbilayer pores through which selected ions may move at high rates ($\sim 10^7$ ions s^{-1} $channel^{-1}$). To understand the physical basis of their functional properties, we need to characterize their structural and dynamic properties. However, this is far from easy. As ion channels are membrane proteins, we know relatively little about their three-dimensional structures. Indeed, although membrane proteins are thought to make up ~20–30% of most genomes (Boyd et al., 1998; Wallin and von Heijne, 1998), we know the high-resolution three-dimensional structure of only a handful of such proteins, including a bacterial K^+ channel (Doyle et al., 1998). Given such relative ignorance, the study of simple model membrane proteins can provide valuable information on membrane protein structure and dynamics. This has proved to be the case for ion channels, where studies of a simple channel-forming peptide, gramicidin A, have provided unique insights into the structural basis of channel function. However, the structural peculiarities of gramicidin are such that it is useful to also examine other peptide models that more closely mimic ion channel proteins. Many ion channels are thought to contain a central pore lined by a bundle of approximately parallel α-helices. Such channels range in complexity from the M2 protein of influenza A (~100 amino acids per subunit) to the nicotinic acetylcholine receptor (~500 amino acids per subunit). Given the importance of this structural motif in channel proteins, it is important to have a simple yet detailed model system for channels formed by α-helices.

Alamethicin (Alm) is a 20-residue peptide that forms ion channels in lipid bilayers. The channel, structural, and spectroscopic properties of Alm have been studied in considerable detail (Woolley and Wallace, 1992; Sansom, 1993; Cafiso, 1994). It forms multiconductance channels in a voltage-dependent manner. The alamethicin molecule adopts a largely α-helical conformation, in the crystal, in nonaqueous solvents, and in the presence of lipid bilayers. This conformation is stabilized by the presence of a large number of Aib residues in the sequence of Alm: Ac-Aib-Pro-Aib-Ala-Aib-Ala-Gln^7-Aib-Val-Aib-Gly-Leu-Aib-Pro^{14}-Val-Aib-Aib-Glu^{18}-Gln-Phol.

The multiconductance behavior of Alm channels is generally explained in terms of the "barrel stave" model (Baumann and Mueller, 1974; Fox and Richards, 1982; Mathew and Balaram, 1983b; Boheim et al., 1983), in which multiple Alm molecules form a helix bundle surrounding a central pore. Different conductance levels correspond to different numbers of helices in the bundle. This model is in accord with a large body of experimental data (reviewed in Sansom, 1993) including neutron scattering studies from Alm in lipid bilayers (He et al., 1995). A key feature of this model is that the helices are oriented parallel (rather than antiparallel) to one another, their helix dipole repulsions being overcome by their favorable interaction with the electrostatic field across the bilayer, and with the water inside the transbilayer pore (Breed et al., 1996). This is supported by the asymmetry of voltage activation of Alm channels. Thus when Alm is added to one face (the *cis* face) of a bilayer, only *cis*-positive voltages will result in channel formation. This argues for a structure that is asymmetrical relative to the bilayer plane, i.e., a parallel helix bundle. Such a structure is supported by the work of Woolley and

Received for publication 15 July 1998 and in final form 8 January 1999.
Address reprint requests to Dr. Mark S. P. Sansom, Laboratory of Molecular Biophysics, Department of Biochemistry, The Rex Richards Building, University of Oxford, South Parks Road, Oxford OX1 3QU, England. Tel.: +44-1865-275371; Fax: +44-1865-275182; E-mail: mark@biop.ox.ac.uk.

0006-3495/99/04/1757/13 $2.00

his colleagues (You et al., 1996; Woolley et al., 1997), who have shown that channels formed by covalently coupled pairs of Alm helices (which are physically constrained to be parallel to one another) strongly resemble channels formed by unmodified Alm.

Molecular models of channels formed by Alm helix bundles have been generated by restrained molecular dynamics (MD) simulations in vacuo, and these models have been refined by short MD simulations with water molecules included within and at each mouth of the pore (Breed et al., 1997a). These models can explain the change in stability of Alm channels when the Gln^7 side chain is replaced by a smaller polar residue (Molle et al., 1996; Breed et al., 1997b). The pore dimensions of such models with different numbers of helices per bundle correlate with the experimentally observed multiple conductances of Alm (Sansom, 1991, 1993; Smart et al., 1997). Similar models of channels formed by Alm analogs have been used as the basis of simple electrostatic calculations that predict with reasonable accuracy the ionic-strength-dependent nonlinear current-voltage curves observed for such channels (Woolley et al., 1997). Models of Alm helix bundles have been used in MD simulations to demonstrate that water within channels formed by parallel helix bundles is ordered and shows reduced translational and rotational mobility relative to bulk water. Finally, models of Alm channels have been used to explore changes in the translational mobility of Na^+ ions when within narrow pores. Thus α-helix bundle models of Alm channels have been studied in some detail and so seem reasonable as the basis of prolonged MD simulations of an α-helix bundle in a lipid bilayer.

In this paper we present the results of 2-ns MD simulations of a hexameric bundle of Alm helices in a 1-palmitoyl-2-oleoylphosphatidylcholine (POPC) bilayer. We explore the stability and conformational dynamics of the bundle in a phospholipid bilayer. We also investigate the effect on bundle stability of the ionization state of the ring of Glu^{18} side chains, and we examine the structural and dynamic properties of water in this channel model.

METHODS

Starting model of hexameric Alm bundle

An initial model of a hexameric Alm helix bundle was generated using restrained MD in vacuo as described by Kerr et al. (1994) and Breed et al. (1997a). During the final stage of the simulated annealing protocol used to build the model, the restraints applied were 1) intrahelix restraints, to maintain H-bonding of the backbone of each Alm monomer, and 2) interhelix restraints, between the N-terminal segments of adjacent monomers of the bundle, to maintain the integrity of the bundle. This model was then solvated, within and at either mouth of the pore. Subsequently 300 ps of in vacuo MD was run, using the protocol described by Breed et al. (1996), to relax polar side-chain conformations within the pore in the presence of water. The same intra- and interhelix restraints were retained during this simulation. The Cα RMSD from the initial in vacuo model to the model at the end of 300 ps in water was $\sim$0.2 nm. The resultant model was then desolvated and used as the starting model for the bilayer simulations.

Two simulation systems

Two simulations of a hexameric Alm helix bundle were run, differing in the ionization state of the Glu^{18} residues. Electrostatic calculations on rings of glutamate residues at either mouth of a model of the pore domain of the nicotinic acetylcholine receptor (Adcock et al., 1998) suggest that $\sim$50% of the glutamates in the C-terminal ring are protonated at neutral pH. It was suspected that a similar suppression of ionization of Glu^{18} might occur in Alm helix bundles. So the ionization states of the Glu^{18} side chains in the Alm bundle models were estimated via pK_A calculations, as described in detail by Adcock et al. (1998). Briefly, intrinsic pK_A values were calculated using

$$pK_{A,INTRINSIC} = pK_{A,MODEL} - \frac{1}{2.303}[\Delta\Delta G_{BORN} + \Delta\Delta G_{BACK}]$$

where $pK_{A,MODEL}$ is the pK_A of an isolated amino acid, $\Delta\Delta G_{BORN}$ is the solvation contribution to the pK_A shift, and $\Delta\Delta G_{BACK}$ is the contribution due to the interaction of the residue with nontitrating charges (Bashford and Karplus, 1991; Karshikoff et al., 1994). Absolute pK_A values were obtained via calculation of titration curves. The latter were obtained via calculation of

$$p(\mathbf{x}) \propto \exp\left[-\ln 10 \sum_i \gamma_i(pK_{A,INTRINSIC,i} - pH) - \beta \sum_i \sum_{k<i} \Delta\Delta G_{i,k}\right]$$

where $p(\mathbf{x})$ is the probability of a residue existing in its ionized state and $\mathbf{x}$ is an N-element state vector whose elements are 0 or 1, depending on whether the residue is un-ionized or ionized, respectively, where $\gamma = -1$ for a basic residue, $\gamma = +1$ for an acidic residue, and $\Delta\Delta G_{i,k}$ is the screened Coulombic interaction energy between pairs of ionizable residues i and k (Bashford and Karplus, 1991; Lim et al., 1991). Results of such pK_A calculations for a hexameric Alm helix bundle suggest that, at pH 7, either none or just one of the six glutamate side chains will be ionized (Tieleman et al., 1998a). So, to investigate the effect of ionization of glutamate side chains on the dynamics and stability of the Alm helix bundle, we have chosen to simulate two limiting states of the system. In one (henceforth referred to as N6), all six glutamates are ionized. In the other (henceforth referred to as N6H), all six glutamates are protonated. We anticipate that the true state of the system is probably closer to N6H than to N6.

The setup of the system will be described first for N6. An equilibrated POPC bilayer with 128 lipid molecules was used. A cylindrical hole was made in the center of the bilayer by removing lipids whose P atoms fell within 1.55 nm of the central axis of the cylinder. A short MD simulation with a radially acting repulsive force was used to drive any remaining atoms out of the cylinder and into the bilayer. The Alm N6 model was inserted into the cavity thus created. This system (N6 plus POPC) was solvated with SPC waters (~30 waters per lipid molecule). Six Na^+ ions replaced water molecules at the positions of lowest Coulomb potential. This was achieved by removal of successive water molecules, one at a time, and calculation of the Coulombic interaction energy of a Na^+ ion at that position with the remainder of the system. The resultant system (6 Alm helices, 3528 waters, 6 Na^+ ions, giving a total of 17,000 atoms in a box of dimensions $6.1 \times 6.1 \times 7.0$ nm^3) was simulated for 10 ps with no restraints, with constant surface area, and with a constant pressure of 1 bar in the z (i.e., bilayer normal) direction, followed by 5 ps with positional restraints on the peptide atoms relative to the starting N6 structure. The N6H system was generated by taking the N6 system thus generated, protonating the six Glu^{18} residues and removing the Na^+ ions. The resultant N6H system was then energy minimized before use in MD. A snapshot of the N6H system is given in Fig. 1.

MD simulation details

Molecular dynamics simulations were run using GROMACS (Berendsen et al., 1995). A twin range cutoff was used for longer-range interactions: 1.0 nm for van der Waals interactions and 1.8 nm for electrostatic interactions. The time step was 2 fs, using SHAKE to constrain bond lengths. We used NPT conditions (i.e., constant number of particles, pressure, and temperature) in the simulation. A constant pressure of 1 bar in all three directions was used, with a coupling constant of $\tau_P = 1.0$ ps (Berendsen et al., 1984). This allows the bilayer/peptide area to adjust to its optimum value for the force field employed. Water, lipid, and protein were coupled separately to a temperature bath at 300 K, using a coupling constant $\tau_T = 0.1$ ps.

The lipid parameters were as in previous MD studies of dipalmitoylphosphatidylcholine bilayers (Berger et al., 1997; Marrink et al., 1998) (with the addition of some GROMOS parameters for the double bond in the acyl tail), and as in our previous paper on MD simulations of a monomeric Alm helix inserted in a POPC bilayer (Tieleman et al., 1999). These lipid parameters give good reproduction of the experimental properties of a dipalmitoylphosphatidylcholine bilayer. The lipid-protein interactions used GROMOS parameters. The water model used was SPC (Berendsen et al., 1981), which has been shown to be a

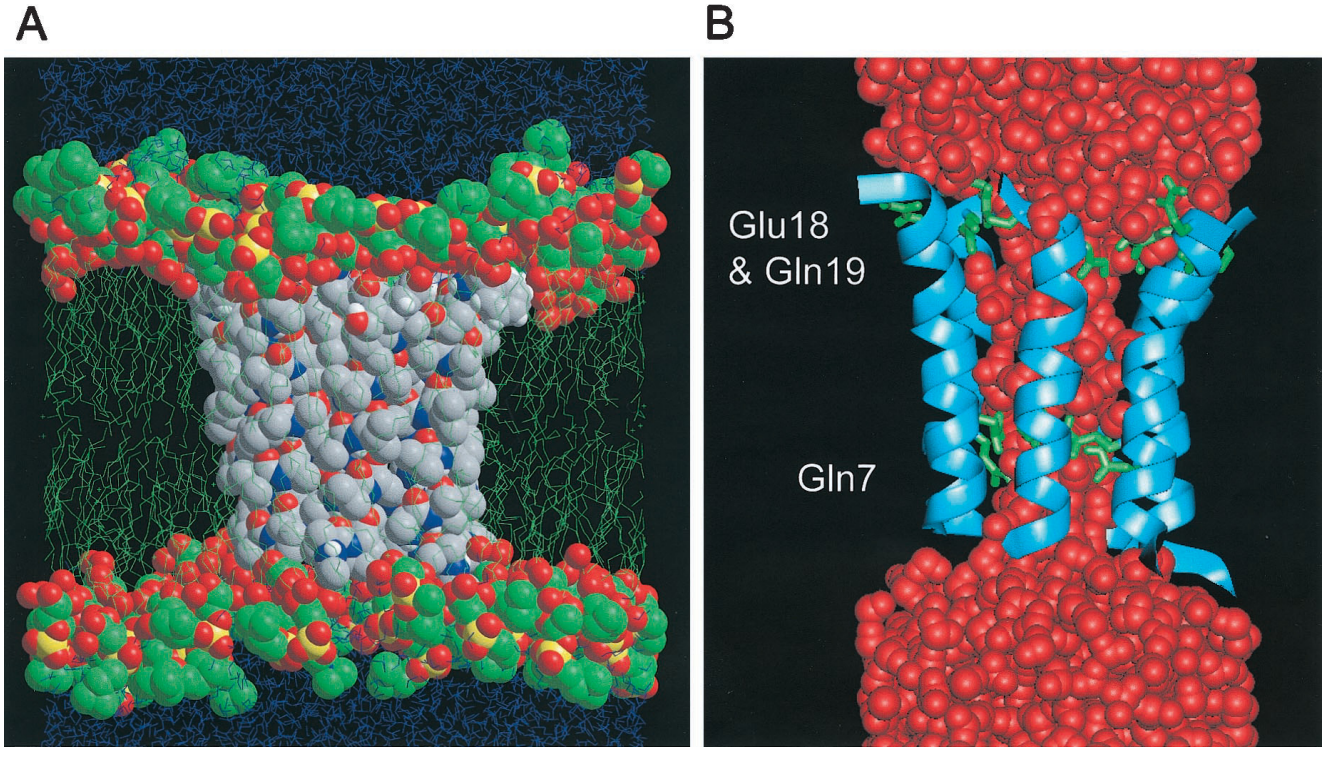

FIGURE 1 (*A*) Starting configuration of the simulation system for an Alm hexameric helix bundle (*cpk colors*) inserted in a POPC bilayer (*green*) with water (*cyan*) on either side. The carbonyl oxygen atoms of the acyl chains of the lipid molecules and the Alm molecule are shown in space-filling format. (*B*) Snapshot of the Alm N6H simulation showing the helix bundle (*blue, in ribbon format*), the rings of Gln^7, Glu^{18}, and Gln^{19} side chains (*green, in stick format*), and water molecules (*red, in space-filling format*) within the pore and extending to either side of the mouths of the pore.

reasonable choice for lipid bilayer simulations (Tieleman and Berendsen, 1996).

Longitudinal diffusion coefficients of water molecules within the pore were determined from their mean square displacement along the pore (z) axis over a period of 5 ps, as described by Tieleman and Berendsen (1998). The diffusion coefficient was assigned to the local region on the pore axis corresponding to the position of the water molecule at the start of the 5-ps period.

Computational details

Simulations were carried out on a 195-MHz R10000 Origin 2000 and took ~8 days per processor per nanosecond of simulation time. This is somewhat faster than other MD codes. In part, this reflects the inclusion of an efficient method for neighbor searching, plus the use of a preprocessor to aid in code optimization. Analysis was performed using facilities within GROMACS and with code written specifically for this project. Secondary structure analysis employed the DSSP algorithm (Kabsch and Sander, 1983). Essential dynamics and domain motion analysis (using DYNDOM) were performed as described by Hayward and Berendsen (1998). Initial models were generated using Xplor (Brünger, 1992) and Charmm (Brooks et al., 1983). pK_A calculations were performed using UHBD version 5.1 (Davis et al., 1991) (with some local modifications) and partial atomic charges from the Quanta/Charmm22 parameter set. Structures were examined using Quanta (Biosym/MSI) and Rasmol, and diagrams were drawn using MolScript (Kraulis, 1991). Pore radius profiles were determined using HOLE (Smart et al., 1993).

RESULTS

Progress of the simulations

The overall progress of the N6 and N6H simulations may be compared via their Cα RMSDs versus time (Fig. 2). For N6 it can be seen that the RMSD increases steadily up to ~0.35 nm over the first 1200 ps or so and then plateaus at this value. This suggests that substantial changes in the structure of the N6 helix bundle occur over the course of the 2-ns simulation. In contrast, the Cα RMSD for the N6H model reaches a peak of ~0.25 nm after 400 ps and then settles at ~0.23 nm for the remainder of the simulation. This suggests that N6H shows substantially smaller structural drift than does N6, and thus that the former protonated state of the hexameric Alm helix bundle is a more stable structure in this MD simulation.

The fluctuations in the dimensions of the simulation box were analyzed as a function of time (data not shown). No significant difference was seen between the N6 and N6H simulations. In both cases the maximum shift from the initial value of any box dimension was ~0.2 nm. In simulation N6 one of the six Na^+ ions moved to associate with one of the Glu^{18} side chains. A second Na^+ ion interacted with O atoms of the lipid headgroups. The other four Na^+ ions remained in the bulk water region of the system. Thus some degree of neutralization of the charge-charge repulsions of the Glu^{18} ring was obtained by inclusion of the Na^+ ions, but this was clearly incomplete.

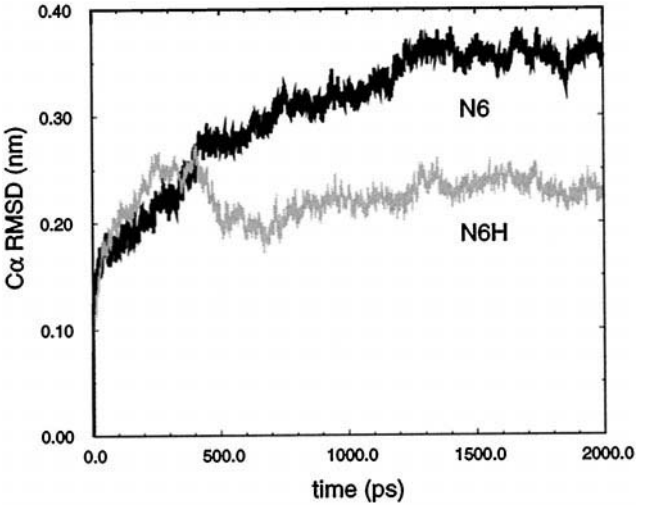

FIGURE 2 RMSDs versus time for the Cα atoms of each simulation: Alm N6 (*black line*) and Alm N6H (*gray line*).

Intrahelix fluctuations and secondary structure

In Fig. 3 the Cα RMS fluctuations (from the mean structure over the course of the simulation) are shown as a function of residue number. The most striking general trend is that the RMS fluctuations are greater for the C-terminal segments of the helices than for the N-terminal segments. If one com-

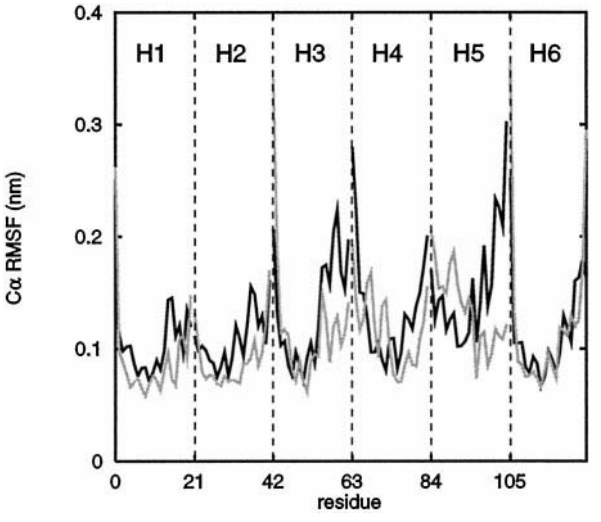

FIGURE 3 Residue-by-residue Cα RMS fluctuations about their average coordinates: Alm N6 (*black line*) and Alm N6H (*gray line*). The vertical broken lines delineate the extents of helices H1 (residues 0–20) to H6 (residues 105–125). (Note that in our residue numbering scheme, residues 0, 21, 42, 64, 84, and 105 correspond to the N-terminal acetyl groups of the Alm molecules.)

pares the magnitude of the fluctuations with those from simulations of a single Alm helix, then they are greater for N6(H) than for a single helix, either inserted in a POPC bilayer or in solution in MeOH, but less than the fluctuations of a single Alm helix in water. Thus the environment of an Alm helix within a helix bundle may be viewed as intermediate between a hydrophobic and an aqueous environment, and the magnitude of its fluctuations is between those found in these two environments. For a majority of the helices (i.e., H1, H2, H3, H4, and H5) the RMS fluctuations of the C-terminal segment are significantly greater for N6 than for N6H.

A similar pattern emerges from analysis of the secondary structures of the constituent helices of the two bundles as functions of time (Fig. 4). Overall, each peptide molecule retains a largely α-helical conformation throughout the 2 ns. In all cases, there is greater deviation from α-helicity, and from a fixed secondary structure, in the C-terminal segments than in the N-terminal of the constituent monomers. The overall level of fluctuation in secondary structure is possibly a little lower for N6 than for N6H, but the difference is not striking. Comparison with fluctuations in the secondary structure of an isolated Alm helix reveals that in the hexameric bundles, the fluctuations in the secondary structure of the C-terminal segment are intermediate in magnitude between those of the isolated helix in an apolar environment and in an aqueous environment. This mirrors the conclusion reached on the basis of the Cα RMSFs (see above). Looking in more detail at the secondary structure, there is some evidence for formation of 3_{10} helix in the C-terminal half of the peptide molecule (e.g., N6, helix H1, $t \approx 1000$ ps, and N6H, helix H5, $t = 1200$–2000 ps). There is obvious variation from helix to helix within a bundle (e.g., helix H4 versus H5 in N6; helix H3 versus H4 in N6H), implying that the helix bundle does not exhibit exact sixfold symmetry. Again, comparison of N6 and N6H suggests a somewhat greater degree of structural fluctuation in the former.

The time-averaged backbone dihedral angles (also averaged over the six helices of each bundle) for the two simulations are shown in Fig. 5. Interestingly, these show almost exactly the same pattern as for MD simulations of an isolated Alm helix in MeOH or inserted in a POPC bilayer (Tieleman et al., 1999). Thus, although the fluctuations of the C-termini of the helices are greater in the pore than in isolated Alm in an apolar environment, the average confor-

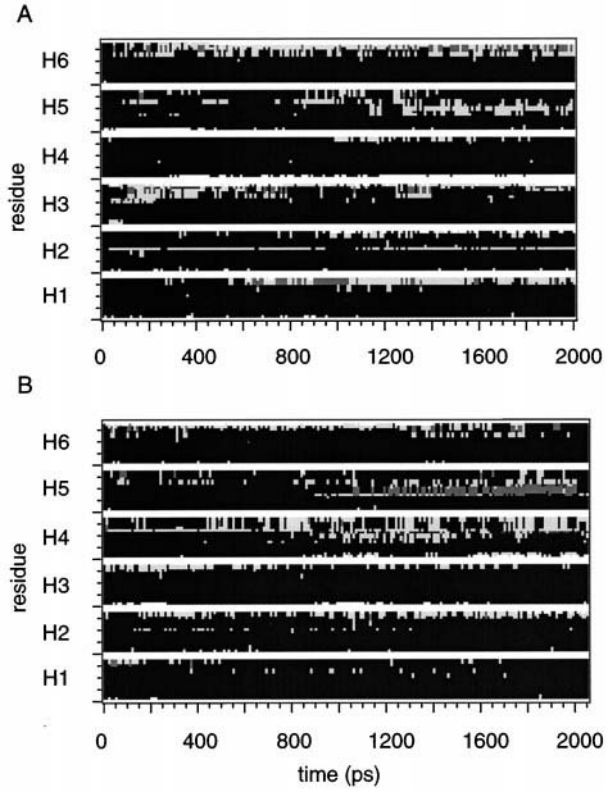

FIGURE 4 Secondary structure, as defined by DSSP (Kabsch and Sander, 1983), as a function of time for Alm N6 (*A*) and Alm N6H (*B*). The gray scale is as follows: black, α-helix; dark gray, 3_{10}-helix; pale gray, turn; white, coil. H1–H6 denote the constituent helices of the bundles.

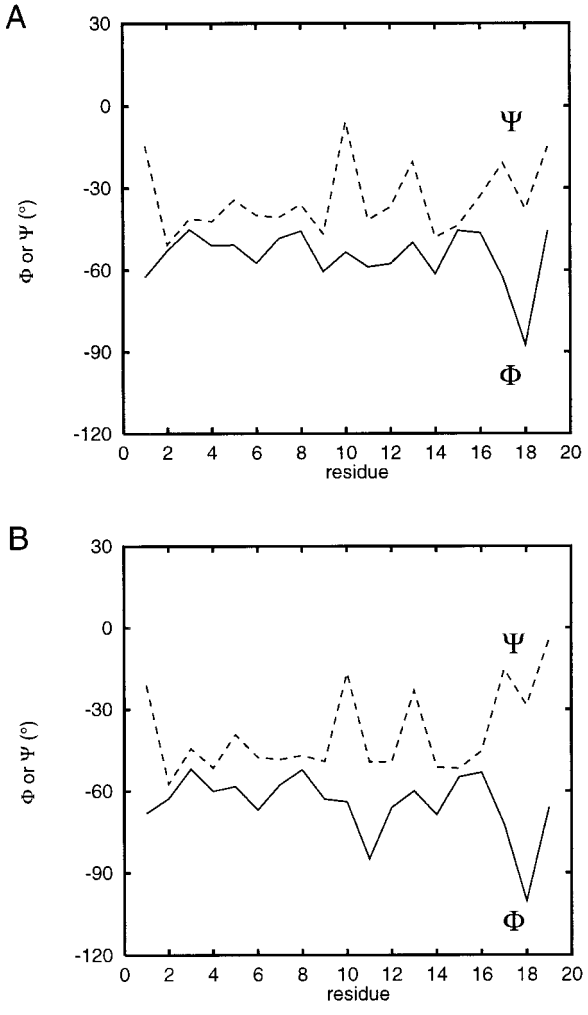

FIGURE 5 Time-averaged values of backbone Φ (——) and Ψ (– – –) angles versus residue number, for all of the helices of Alm N6 (*A*) and Alm N6H (*B*).

mation is the same. This differs from isolated Alm in water, where different values of the mean dihedrals are seen. Thus Alm molecules in a water-filled bundle exhibit greater amplitude motions than they do in a less polar environment, but retain the same average conformation .

Possible hinge-bending motions of Alm molecules within the hexameric bundles were explored in detail by combining essential dynamics (Amadei et al., 1993) with the DYNDOM analysis of Hayward and Berendsen (1998) to reveal the major components of intramolecular motions. However, the results of this analysis were complex. Greater intramolecular mobility is seen for the N6 simulation than for the N6H. However, the analysis did not reveal the hinge-bending-type motion that we have previously encountered within isolated Alm helices, both in MeOH and when inserted (not in bundles) in a POPC bilayer. Rather, the motion involved twisting as well as bending and differed in detail between the six helices of a bundle. However, in general, for example, N6H residues ~1–11 and 14–20 do tend to act like more rigid domains, with flexibility being associated mainly with the Gly-X-X-Pro motif. Thus the environment experienced by Alm molecules within a helix bundle, in which they are exposed to both lipid and water, results in more complex patterns of motion than those seen for isolated helices.

Bundle fluctuations

It seems that the C-terminal segments of the component helices show greater intramolecular fluctuations for N6 than for N6H. Together with the difference seen in the Cα RMSDs, this suggests that the stability of the bundle per se might also differ between N6 and N6H. This is supported by visual examination of Cα trace snapshots of the N6 and N6H bundles taken at 500-ps intervals along each trajectory (Fig. 6 *A–D*). The N6 bundle appears to expand somewhat as time progresses. This is confirmed by comparison of the radius of gyration as a function of time for the two systems (Fig. 7). Changes are particularly evident for the C-terminal segments of the helices, the packing of which is considerably disrupted (relative to the starting model), to allow the charged Glu^{18} side chains to move away from one another. In particular, as a consequence of such changes in packing, one helix (helix H4) no longer seems to have its N-terminal segment packed with those of its neighbors. In contrast, in simulation N6H, the N-terminal segments of the helices remain packed with one another, much as in the initial model. The differences in the interactions can also been seen in the orientations of the Glu^{18} side chains (Fig. 6, *E* and *F*). In N6H these continue to point toward the lumen of the channel, whereas in N6 a number of the (charged) Glu^{18} side chains are pointing away from the channel lumen at the end of the simulation.

Overall, the N6H helix bundle is more stable than the N6 bundle over the duration of the simulation. We will now examine the nature of the H-bonding interactions of the pore with the bilayer and with water, and the behavior of water within the pore in more detail. We will focus on N6H, although some comparisons will be made with N6 to assess the robustness of our conclusions.

Bundle interactions

The amphipathic Alm helices in the bundle are in an anisotropic environment, with their apolar side chains directed toward the surrounding lipids and their polar side chains toward the water within the pore. Furthermore, the polar residues at the C-termini of the helices (i.e., $Glu(H)^{18}$, Gln^{19}, and the terminal hydroxyl of $Phol^{20}$) are close to the lipid headgroups. Comparison of the numbers of H-bonds formed by the Alm helix bundle (simulation N6H) with water molecules (Fig. 8 *A*) and with lipid molecules (Fig. 8 *B*) shows that bundle/water H-bonds predominate. However, a number of peptide/lipid H-bonds do occur, from the side chains of $GluH^{18}$ and Gln^{19} and the terminal hydroxyl of $Phol^{20}$ to the phosphate, glyceryl, and acyl oxygens of the lipid. The number of these H-bonds rises during the first ~800 ps of the simulation (Fig. 8 *D*) until there is about one H-bond to lipid for each Alm helix (a similar pattern is seen for the N6 simulation; data not shown). This is expected to contribute to the stability of the helix bundle, by helping to "anchor" it to the lipid bilayer.

Given the preponderance of peptide/water H-bonds and the crucial role these must play in stabilizing a pore (as opposed to a "closed" bundle of helices), it is important to examine these in more detail to identify the relative contributions of the polar residues of the Alm helix to the lining of the pore. Let us first look at the H-bonds to water molecules of the Gln^7 side chains (Fig. 8 *C*). Gln^7 was first suggested to play a role in stabilizing the Alm helix bundle when the x-ray structure of Alm was determined (Fox and Richards, 1982; Mathew and Balaram, 1983a). More recently, combined experimental and computational studies have supported a role for this side chain in pore stabilization (Molle et al., 1996; Breed et al., 1997b). Counting the number of H-bonds to water made by this side chain reveals that between 20 and 25 H-bonds per hexameric bundle (i.e., about four H-bonds per side chain) are maintained throughout the N6H simulation. Similar behavior is seen for N6 (not shown). Thus the Gln^7 side chains maximize their H-bonding to water within the pore. Moving along the Alm helix, it has been suggested (Sansom, 1992) that the proline-induced helix kink exposes the backbone carbonyl oxygen atoms of Aib^{10} and Gly^{11}, thus enabling these backbone groups to contribute to the polar lining of the pore. Enumeration of H-bonds reveals that this is indeed the case, although it seems that the Aib^{10} carbonyl (Fig. 8 *D*) is rather more solvent-exposed than is that of Gly^{11} (Fig. 8 *E*).

The (protonated) Glu^{18} side chains maximize their H-bonding to pore water (Fig. 8 *F*). The side chains of Gln^{19} (Fig. 8 *G*) also form a significant number of H-bonds to water. Taken together, these two rings of side chains con-

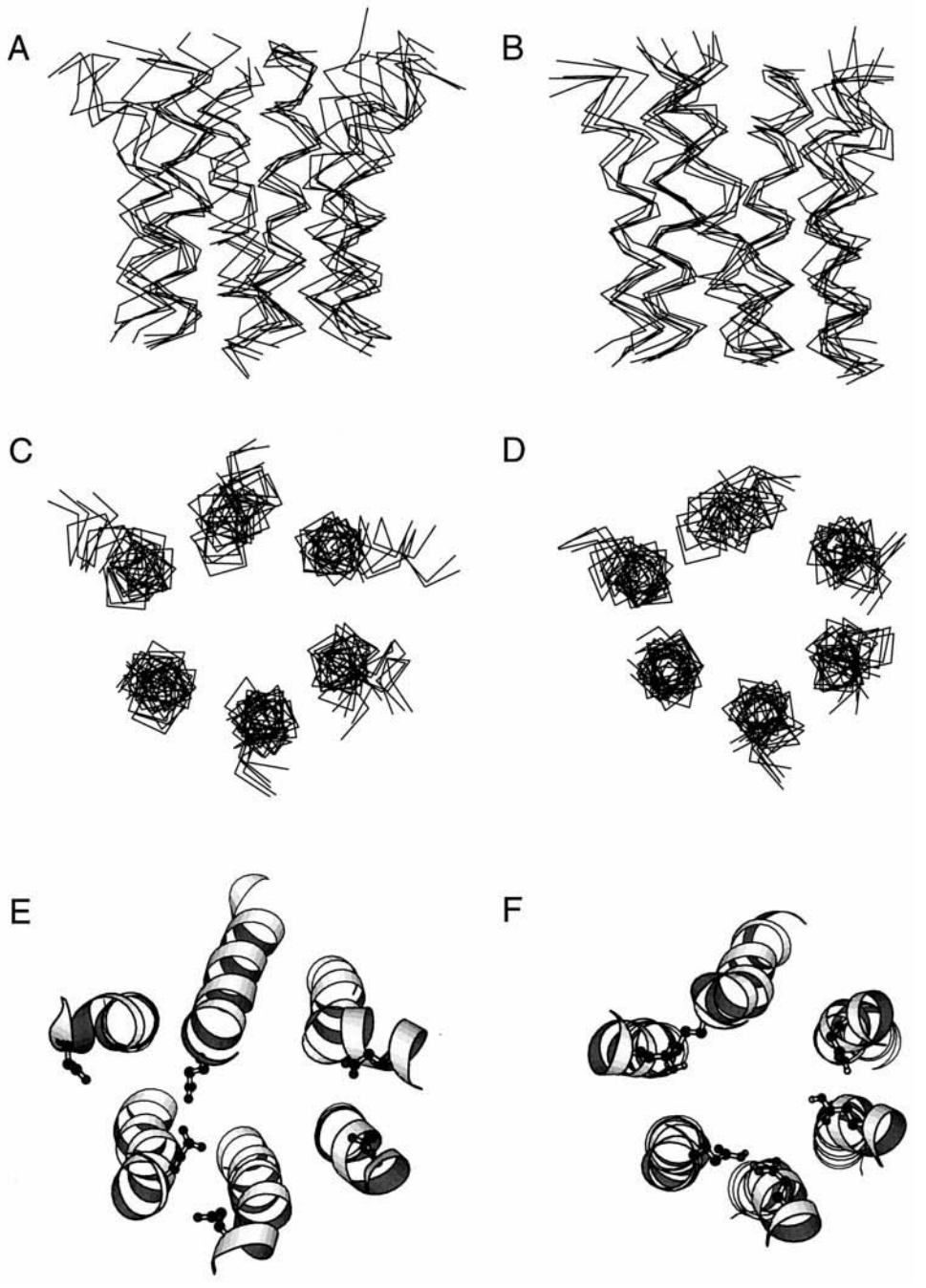

FIGURE 6 (*A–D*) Cα traces of snapshots (at 0, 500, 1000, 1500, and 2000 ps) from the Alm N6 (*A,C*) and Alm N6H (*B,D*) simulations. In *A* and *B* the helix bundles are viewed down a perpendicular to the bilayer normal, with the C-termini of the helices uppermost. In *C* and *D* the view is from the C-terminal mouth of the pore, down the bilayer normal. (*E,F*) Structures of the Alm N6 (*E*) and Alm N6H (*F*) simulations at $t = 2000$ ps.

tribute ~30 H-bonds to water throughout the simulation. Finally, the C-terminal hydroxyl group of Phol[20] (Fig. 8 *H*) forms about two H-bonds to water per Alm monomer. Interestingly, the numbers of side chain/water H-bonds for the N6H bundle do not vary greatly with respect to time, whereas the corresponding numbers for the less stable N6 bundle (data not shown) show significant drift as the helices move apart.

The overall view that emerges is that the amphipathic nature of the Alm helix bundle is ideal for an ion channel. The polar interior interacts strongly with water within the pore, the apolar exterior interacts favorably with the lipid, and there are also some peptide/lipid H-bonds in the "interfacial" region.

The pore and its water

As seen in previous simulation studies (in the absence of a bilayer (Breed et al., 1996)) there is a well-defined column of water within the lumen of the Alm helix bundle (Fig. 9). At its narrowest region, in the vicinity of the Gln[7] ring, this accommodates only four or five water molecules. As the water within a pore is crucial to the permeation of ions

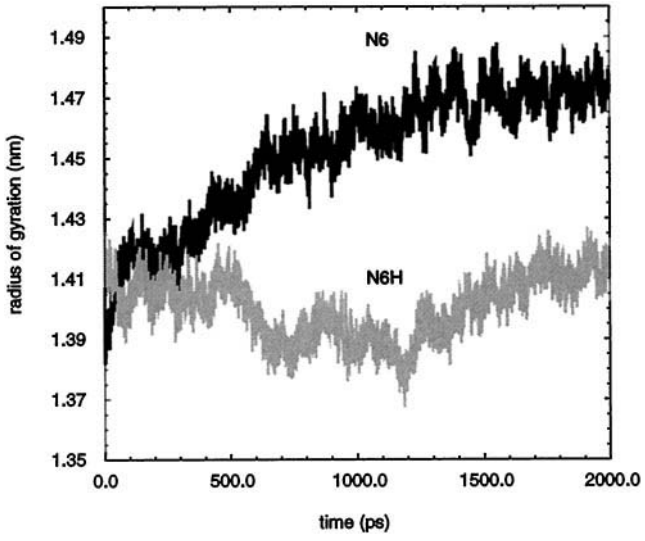

FIGURE 7 Radius of gyration as a function of time for the Alm N6 (*black line*) and Alm N6H (*gray line*) simulations.

through that pore, we have examined the nature of the pore and its water in some detail. The pore radius profile has been determined every 50 ps. The resultant time-averaged radius profiles for N6 and N6H are compared in Fig. 9 *A*. Despite the lesser stability of the N6 bundle, the profiles are relatively similar. That of N6H has a smaller minimum radius, as might be expected, given the expansion of the N6 bundle noted above. There are two constrictions, the narrower one being in the vicinity of the Gln^{7} ring and the slightly wider one in the vicinity of the $Glu(H)^{18}$ ring. At its narrowest point the pore has a radius of ~0.25 nm, and so partial dehydration of, e.g., a K^+ ion (ionic radius 0.13 nm) may occur in this region during permeation, although it should be remembered that the Gln^{7} side chains may exhibit flexibility. On the basis of this pore radius one may obtain an approximate prediction of the pore conductance using the methods of Smart et al. (1997). For 1 M KCl this yields a predicted single-channel conductance of 260 pS, which is in agreement with the corresponding experimental value of 280 pS (Hanke and Boheim, 1980; Smart et al., 1997).

We have examined the longitudinal (i.e., along the pore z axis) diffusion coefficient of water molecules in the system as a function of their z coordinate (see Fig. 9 *B*). Note that those waters within the pore are located between $z = 1.5$ and $z = 4.5$ nm. The diffusion coefficients of waters within the pore are markedly reduced relative to those of waters in the "bulk" region. Note that the "bulk" diffusion coefficient of SPC water is $\sim 5 \times 10^{-9}$ m^2 s^{-1}. In the narrowest region of the pore ($z \approx 2.8$ nm, corresponding to the Gln^{7} ring), the water diffusion coefficient falls to $\sim 0.4 \times 10^{-9}$ m^2 s^{-1}, i.e., ~1/12 of its bulk value. Thus the substantial reduction in the translational motion of water within narrow pores seen in simpler simulations (Breed et al., 1996) is reproduced in the current, more realistic study. The motion of water is also reduced close to the surface of the bilayer, i.e., at $z \approx 1.0$ nm and $z \approx 5$ nm (Marrink and Berendsen, 1994; Tieleman and Berendsen, 1996).

The dipoles of the water molecules within the pore are oriented by the helix dipoles (Fig. 9 *C*). Thus, within the pore the mean z component of the water dipoles is nearly 2.0 Debye, which should be compared with a dipole moment of 2.3 Debye for a single SPC water. Much the same orientation of water dipoles within the pore is seen whether one analyses N6H (no ionized side chains) or N6 (six ionized side chains). However, in the latter case there is some local orientational polarization of the water dipoles in the vicinity of the Glu^{18} ring superimposed upon the overall orientational polarization due to the helix dipoles. Given the differences in helix packing (less ordered) in the N6 simulation, this suggests that this effect of the helix dipoles on the water is robust to the details of the model and so might be expected to be a general feature of those ion channels whose pores are formed by bundles of approximately parallel α-helices.

The observed degree of orientation of the water dipoles may be employed to calculate the local field experienced by water molecules within the pore. (Note that we anticipate that this field will not be as strong outside the helix bundle, where the reinforcing effects of the multiple helix dipoles will not be experienced as strongly.) Thus the maximum value of $\mu_z = 1.9$ Debye in the middle of the pore (Fig. 9 *C*) should be compared with $\mu_0 = 2.3$ Debye for SPC water (where μ_0 is the dipole moment of water and μ_z is its projection along the z (pore) axis). Using the Langevin equation

$$\mu_z = \mu_0 \left[\coth\left(\frac{\mu_0 E_z}{k_B T}\right) - \left(\frac{k_B T}{\mu_0 E_z}\right) \right]$$

where E_z is the z component of the electrostatic field due to the helix dipoles, and k_B and T are the Boltzmann constant and temperature, respectively, this yields a field $E_z = 3.4 \times 10^9$ Vm^{-1}. (See (Sansom et al., 1997b) for a more detailed description of the theory of interaction of α-helix bundle dipoles with pore water molecules.) This "observed" field must be compared with an approximate prediction of the electrostatic field generated by the bundle of aligned α-helix dipoles. An estimate of the latter field was obtained by numerical differentiation of the electrostatic potential energy along the pore axis of an Alm helix bundle in vacuo. To obtain the electrostatic potential along the pore axis, just the backbone atoms (with Charmm partial atomic charges) were used, although inclusion of side-chain atoms did not make a significant difference as long as the negative charges on the carboxylates of the glutamate residues were omitted. Note that this approximate prediction is a simple Coulombic field and does not take into account the environment surrounding the helix bundle. The field estimated in this fashion had a maximum value in the center of the pore of $\sim 1.5 \times 10^9$ Vm^{-1}. This is in good agreement with the "observed" field calculated from the Langevin equation

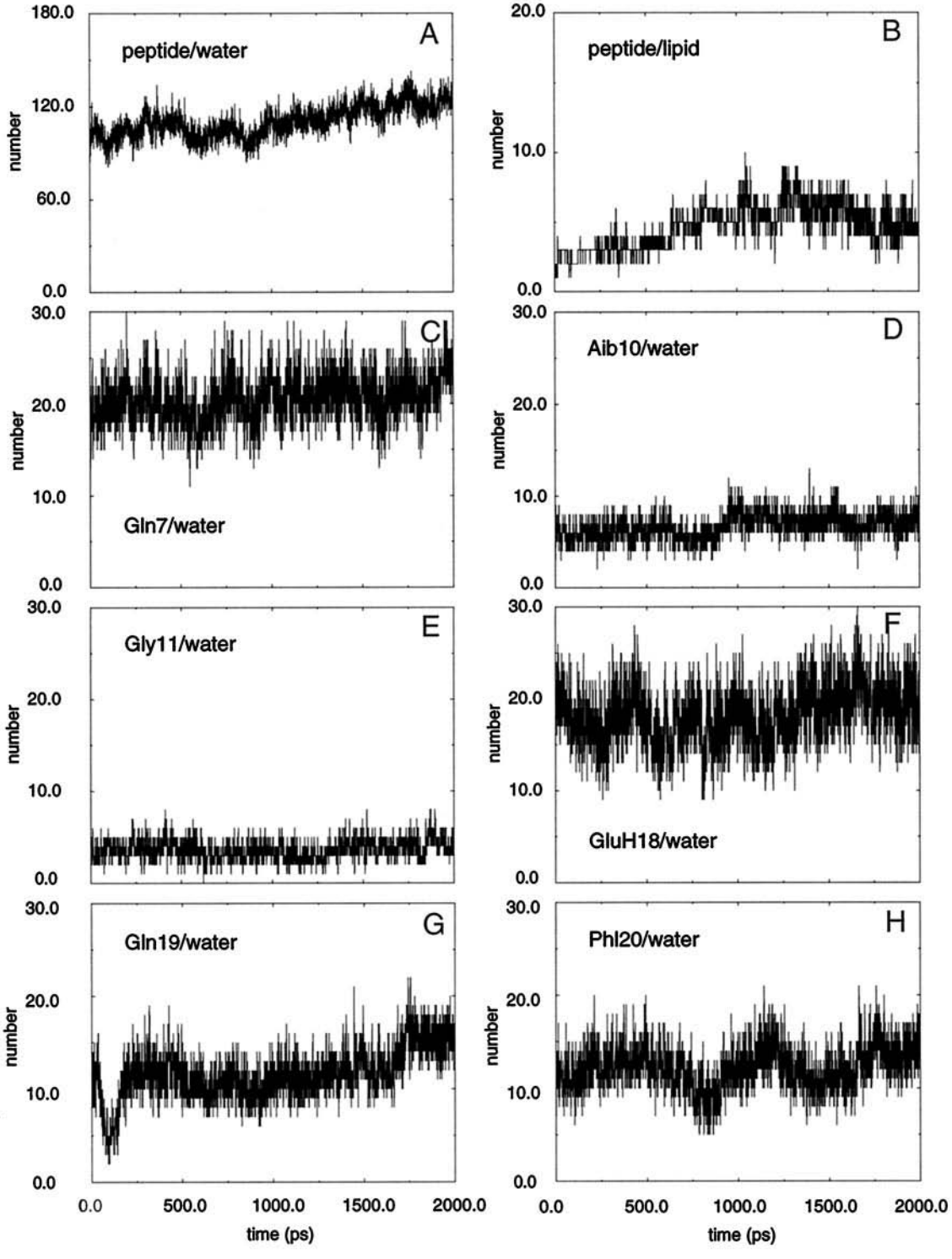

FIGURE 8 Analysis of H-bonding in the Alm N6H simulations. The number of H-bonds as a function of time is shown for (*A*) peptide to water; (*B*) peptide to lipid; (*C*) Gln^{7} side chains to water; (*D*) Aib10 carbonyl oxygen to water; (*E*) Gly^{11} carbonyl oxygen to water; (*F*) $GluH^{18}$ side chains to water; (*G*) Gln^{19} side chains to water; and (*H*) the terminal hydroxyl of $Phol^{20}$ to water.

(given the approximations involved). This agreement confirms that there is indeed a strong interaction between water dipoles and aligned helix dipoles, which will contribute to the stability of the pore. The importance of this interaction may be evaluated by comparing the time-averaged helix-helix electrostatic interaction energy within the N6H bundle ($\sim+140$ kJ/mol) with the corresponding bundle-water electrostatic interaction energy (~-2950 kJ/mol). From this it can be seen that the water-bundle interactions more than compensate for the unfavorable helix-helix interactions, as

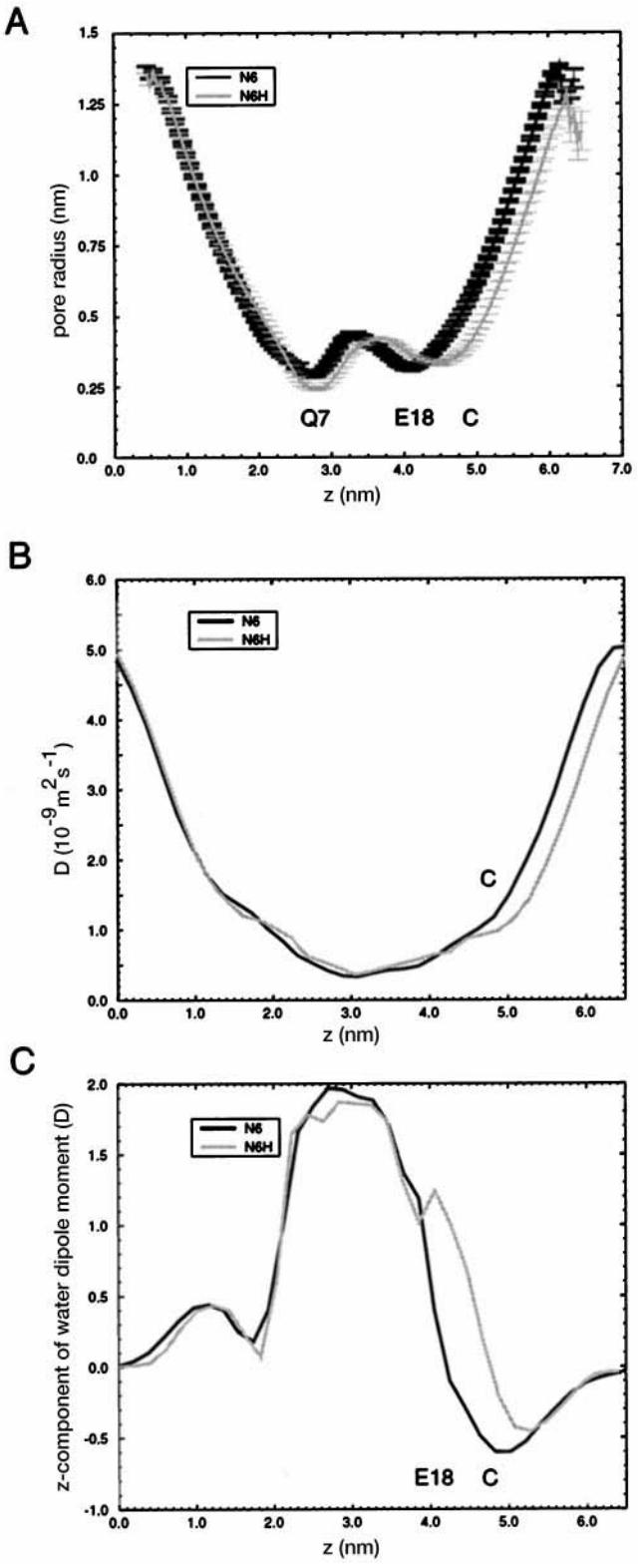

FIGURE 9 (*A*) Pore radius profiles, evaluated using HOLE (Smart et al., 1993), for the Alm N6 (*black line*) and Alm N6H (*gray line*) simulations. The profiles were averaged from structures saved every 50 ps. Error bars represent standard errors. (*B*) Water diffusion coefficients (D_z) as a function of position along the pore (z) axis for the Alm N6 (*black line*) and Alm N6H (*gray line*) simulations. (*C*) Projection of water dipole moments onto the pore axis for the Alm N6 (*black line*) and Alm N6H (*gray line*) simulations.

was suggested by previous in vacuo simulations (Breed et al., 1996).

DISCUSSION

Scope of simulations

This is the first MD simulation of an ion channel formed by a bundle of α-helices to be conducted in a full lipid bilayer. Zhong et al. (1998a,b) have conducted simulations on bundles of the de novo designed α-helices of Lear et al. (1988) and Åkerfeldt et al. (1993), but these were conducted using a bilayer mimic made up of a slab of octane between two aqueous phases. The experimental properties of Alm and its channels are well known (Sansom, 1993). This facilitates comparison with the properties emergent from the simulations. For example, the single-channel conductance predicted on the basis of the simulated Alm N6H structure is in good agreement with that determined experimentally. Indeed, the agreement is slightly better than that obtained with the earlier, in vacuo model of the Alm hexameric helix bundle. The current simulations are of a reasonable duration (by MD standards). Furthermore, continuum electrostatic calculations have allowed us to pay attention to the likely ionization states of the Glu^{19} side chains. In particular, the stability of the Alm N6H bundle during the simulations provides further evidence that this model may be a reasonable approximation to the true structure of (this conductance level of) the alamethicin channel.

However, these simulations remain an approximation to the true properties of the system. In particular, 2 ns is still a relatively short period of time, in the context of both lipid motions (Tieleman et al., 1997) and the mean time it takes an ion to move through a channel (~10–100 ns). Furthermore, the simulations have been conducted in the absence of a transbilayer voltage difference. This is not too serious a problem, as the work of, e.g., He et al. (1995) suggests that Alm helix bundles may form in the absence of such a voltage difference, even though Alm pore formation is voltage dependent at the low peptide:lipid ratios employed in electrophysiological studies. However, a number of recent simulations (Biggin and Sansom, 1996; Biggin et al., 1997; Zhong et al., 1998b) and theoretical (Roux, 1997) studies have explored the modeling of a transbilayer voltage difference, and it will be important to conduct simulations similar to those described in this paper in the presence of such an external electrostatic field. The other major simplification is that only a hexameric bundle of Alm molecules has been considered. Models of smaller ($N = 4$ and 5) and larger ($N = 7$ and 8) Alm helix bundles have been generated in earlier, in vacuo MD studies (Breed et al., 1997a) and will form the basis of future MD simulations in an explicit bilayer plus water environment. There are further limitations to the simulations, such as the absence of electrolyte. Typically, experimental studies of Alm channels are conducted using at least 0.5 M electrolyte, corresponding to ~50 ions in the system used in this simulation. This is an

area that future studies will have to address. Long simulation runs will be required to allow efficient equilibration of such a system. A further limitation is the relatively simple treatment of long-range electrostatic interactions. The simulation protocol we have used has been shown to give reasonable agreement with experimental results for pure bilayer simulations (Tieleman et al., 1997) and to yield stable simulations for the porin OmpF in a POPE bilayer (Tieleman and Berendsen, 1998). However, a number of studies have been concerned with the effects of different treatments of long-range electrostatic interactions (Tobias et al., 1997; Tieleman et al., 1997). It is likely that in the presence of explicit charges long-range interactions should be included by proper lattice sums so as to avoid artefacts.

Biological significance

Despite the limitations of the simulations, the properties of the Alm N6H bundle and of its interactions with water and lipids are of some significance. In particular, the Alm helix bundle may be thought of as a paradigm of other ion channels formed by helix bundles, including the pore domains of the influenza M2 protein proton pore (Sansom et al., 1997a; Forrest et al., 1998) and of the nicotinic acetylcholine receptor (Unwin, 1995; Sankararamakrishnan et al., 1996; Sansom et al., 1998a). Furthermore, the recently determined x-ray structure of a bacterial K^+ channel (Doyle et al., 1998) reveals a pore based upon an α-helix bundle motif, into which the pore-lining P-domain is inserted to confer greater ion selectivity. As it seems likely that this basic architecture will be found in voltage-gated K^+, Na^+, and Ca^{2+} channels (Sansom, 1998), the parallel helix bundle motif may prove to be widespread among a wide range of ion channels.

One property that clearly emerges from the current study is the altered dynamics of water molecules within the pore. This has also been seen in comparable simulations of the bacterial porin OmpF (Tieleman and Berendsen, 1998). Significantly, an almost identical effect on dynamics of water with Alm and other model pores was observed in previous simulations of a pore plus water system in the absence of a bilayer model, i.e., essentially in vacuo (Breed et al., 1996). This is important in that it suggests such simpler simulations may capture the essence of the dynamics of water (and, by extension, of ions; Smith and Sansom, 1997; Smith and Sansom, 1998) in models of transbilayer pores. The other unusual property of water within Alm channels is the alignment of the water dipoles along the pore axis. This was also observed in the earlier simulations (Breed et al., 1996; Mitton and Sansom, 1996), and current calculations demonstrate rather conclusively that the water dipoles are aligned by the electrostatic field created by the parallel dipoles of the constituent α-helices of the bundle. Such alignment of intrapore water dipoles has an important consequence for more mesoscopic treatments of channel properties. As discussed by Sansom et al. (1997b), alignment of the water dipoles by the helix dipoles means that if the water within the pore is modeled as a continuum, a somewhat lower dielectric than that of bulk water should be used. (However, there may be other, rather more fundamental problems in treating nearly dielectrically saturated water as a simple dielectric continuum.) Furthermore, as discussed above, helix/water dipolar interactions contribute to the stabilization of a parallel α-helix bundle.

A further way in which the Alm helix bundle may be of relevance to other ion channels is in the flexibility conferred on the helices by the proline residues at position 14. From the DSSP analysis and from visualization of superimposed structures, it is evident that even in the Alm N6H simulation the C-terminal segments of the Alm molecules undergo dynamic conformational changes. Comparison with simulations of an isolated Alm molecule in water, in MeOH, and spanning a POPC bilayer (Tieleman et al., 1999) suggests that in N6H the degree of conformation flexibility is greater than that of the isolated Alm molecule in a transbilayer (POPC) or bilayer-mimetic (MeOH) environment, but is less than that of Alm in water. This is presumably because in N6H the Alm helices are exposed to water only on the pore-lining surface. Thus the Alm channel is a dynamic assembly, with rapid structural fluctuations around its C-terminal mouth. This is also of interest in the context of K^+ channels. The recent bacterial KcsA channel structure has a bundle of four inner helices that appear to restrict the size of the intracellular channel mouth. The equivalent S6 helices of voltage-gated K^+ channels (e.g., *Shaker*) contain a Pro-Val-Pro motif, which in vacuo MD simulations suggested might act as a hinge-bending motif. Recent MD simulations of isolated S6 helices in a POPC bilayer (Shrivastava et al., unpublished results) suggest that hinge-bending motion occurs within a bilayer environment. Thus K^+ channels may exhibit fluctuations in their pore dimensions similar to those seen in Alm channels.

Taken together, these results give some indication of the level of approximation necessary in simulation to study ion channel function. Water properties appear to be relatively unperturbed by the presence/absence of a lipid bilayer in the simulation. Thus, if one wishes to study the interactions of water (and possibly those of ions) with a pore, it may be sufficient to run simulations in which the pore model is gently restrained (e.g., Cα harmonic restraints), but which omit the lipid environment. However, if one is interested in more dynamic aspects of channel function (e.g., channel gating), it will almost certainly be necessary to include the bilayer environment of the channel. Of course, if ion permeation per se involves local conformational change of the channel (as appears to be the case for gramicidin (Roux and Karplus, 1991) and may be the case for KcsA (Shrivastava and Sansom, unpublished results)), then there is a danger that Cα harmonic restraints may damp such motions. Hence full bilayer-embedded simulations will be needed.

Future directions

This work has demonstrated that MD simulations of Alm including a lipid bilayer plus water enable unrestrained simulations of a channel-forming helix bundle to be carried out in a realistic model of its natural environment. In the context of the large body of experimental data concerning Alm channels (Sansom, 1993), there are a number of ways in which this work may be extended. First, to better understand the energetics of pore/ion interactions, free energy profiles (Roux and Karplus, 1991, 1994; Roux, 1996; Dorman et al., 1996) for the ion as it moves along the pore should be calculated. In this context, the result in the paper suggesting that water dynamics and orientation in the full bilayer simulation are very similar to those in earlier, restrained, and in vacuo simulations may be helpful. Second, simulations should be extended to models of other values of N helices per bundle to see whether the agreement between predicted and experimental pore conductance found in the current study is maintained (Tieleman et al., 1998a). Furthermore, it will be interesting to run longer (e.g., 20 ns; Tieleman and Sansom, unpublished results) simulations to see whether, for example, differences in the structural dynamics between individual helices of the bundle as observed in the current study average out over time. Such extended simulations will also provide better statistics for the analysis of how peptide/lipid interactions may influence the stability of the helix bundle (Tieleman et al., 1998b). Finally, the effects of varying the helix bundle environment, by including a transbilayer voltage term (Biggin et al., 1997; Zhong et al., 1998b) and by exploring different phospholipids, should be explored. In this way it should be possible to build up a complete picture of the dynamics and energetics of an ion channel (Sansom et al., 1999), albeit a simple one.

Work in the laboratory of MSPS is supported by The Wellcome Trust. DPT was supported by the European Union under contract CT94-0124.

REFERENCES

Adcock, C., G. R. Smith, and M. S. P. Sansom. 1998. Electrostatics and the selectivity of ligand-gated ion channels. *Biophys. J.* 75:1211–1222.

Åkerfeldt, K. S., J. D. Lear, Z. R. Wasserman, L. A. Chung, and W. F. DeGrado. 1993. Synthetic peptides as models for ion channel proteins. *Acc. Chem. Res.* 26:191–197.

Amadei, A., A. B. M. Linssen, and H. J. C. Berendsen. 1993. Essential dynamics of proteins. *Proteins Struct. Funct. Genet.* 17:412–425.

Bashford, D., and M. Karplus. 1991. Multiple-site titration curves of proteins: an analysis of exact and approximate methods for their calculation. *J. Phys. Chem.* 95:9556–9561.

Baumann, G., and P. Mueller. 1974. A molecular model of membrane excitability. *J. Supramol. Struct.* 2:538–557.

Berendsen, H. J. C., J. P. M. Postma, W. F. van Gunsteren, A. DiNola, and J. R. Haak. 1984. Molecular dynamics with coupling to an external bath. *J. Chem. Phys.* 81:3684–3690.

Berendsen, H. J. C., J. P. M. Postma, W. F. van Gunsteren, and J. Hermans. 1981. Intermolecular Forces. Reidel, Dordrecht.

Berendsen, H. J. C., D. van der Spoel, and R. van Drunen. 1995. GROMACS: a message-passing parallel molecular dynamics implementation. *Comput. Phys. Comm.* 95:43–56.

Berger, O., O. Edholm, and F. Jahnig. 1997. Molecular dynamics simulations of a fluid bilayer of dipalmitoylphosphatidycholine at full hydration, constant pressure and constant temperature. *Biophys. J.* 72:2002–2013.

Biggin, P., J. Breed, H. S. Son, and M. S. P. Sansom. 1997. Simulation studies of alamethicin-bilayer interactions. *Biophys. J.* 72:627–636.

Biggin, P. C., and M. S. P. Sansom. 1996. Simulation of voltage-dependent interactions of α-helical peptides with lipid bilayers. *Biophys. Chem.* 60:99–110.

Boheim, G., W. Hanke, and G. Jung. 1983. Alamethicin pore formation: voltage-dependent flip-flop of α-helix dipoles. *Biophys. Struct. Mech.* 9:181–191.

Boyd, D., C. Schierle, and J. Beckwith. 1998. How many membrane proteins are there? *Protein Sci.* 7:201–205.

Breed, J., P. C. Biggin, I. D. Kerr, O. S. Smart, and M. S. P. Sansom. 1997a. Alamethicin channels—molecular modelling via restrained molecular dynamics simulations. *Biochim. Biophys. Acta.* 1325:235–249.

Breed, J., I. D. Kerr, G. Molle, H. Duclohier, and M. S. P. Sansom. 1997b. Ion channel stability and hydrogen bonding. Molecular modelling of channels formed by synthetic alamethicin derivatives. *Biochim. Biophys. Acta.* 1330:103–109.

Breed, J., R. Sankararamakrishnan, I. D. Kerr, and M. S. P. Sansom. 1996. Molecular dynamics simulations of water within models of transbilayer pores. *Biophys. J.* 70:1643–1661.

Brooks, B. R., R. E. Bruccoleri, B. D. Olafson, D. J. States, S. Swaminathan, and M. Karplus. 1983. CHARMM: a program for macromolecular energy, minimisation, and dynamics calculations. *J. Comp. Chem.* 4:187–217.

Brünger, A. T. 1992. X-PLOR Version 3.1. A System for X-Ray Crystallography and NMR. Yale University Press, New Haven, CT.

Cafiso, D. S. 1994. Alamethicin—a peptide model for voltage gating and protein membrane interactions. *Annu. Rev. Biophys. Biomol. Struct.* 23:141–165.

Davis, M. E., J. D. Madura, B. A. Luty, and J. A. McCammon. 1991. Electrostatics and diffusion of molecules in solution: simulations with the University of Houston Brownian dynamics program. *Comput. Phys. Comm.* 62:187–197.

Dorman, V., M. B. Partenskii, and P. C. Jordan. 1996. A semi-microscopic Monte Carlo study of permeation energetics in a gramicidin-like channel: the origin of cation selectivity. *Biophys. J.* 70:121–134.

Doyle, D. A., J. M. Cabral, R. A. Pfuetzner, A. Kuo, J. M. Gulbis, S. L. Cohen, B. T. Cahit, and R. MacKinnon. 1998. The structure of the potassium channel: molecular basis of K^+ conduction and selectivity. *Science.* 280:69–77.

Forrest, L. R., W. F. DeGrado, G. R. Dieckmann, and M. S. P. Sansom. 1998. Two models of the influenza A M2 channel domain: verification by comparison. *Folding Design.* 3:443–448.

Fox, R. O., and F. M. Richards. 1982. A voltage-gated ion channel model inferred from the crystal structure of alamethicin at 1.5 Å resolution. *Nature.* 300:325–330.

Hanke, W., and G. Boheim. 1980. The lowest conductance state of the alamethicin pore. *Biochim. Biophys. Acta.* 596:456–462.

Hayward, S., and H. J. C. Berendsen. 1998. Systematic analysis of domain motions in proteins from conformational change: new results on citrate synthase and T4 lysozyme. *Proteins Struct. Funct. Genet.* 30:144–154.

He, K., S. J. Ludtke, H. W. Huang, and D. L. Worcester. 1995. Antimicrobial peptide pores in membranes detected by neutron in plane scattering. *Biochemistry.* 34:15614–15618.

Hille, B. 1992. Ionic Channels of Excitable Membranes, 2nd Ed. Sinauer Associates, Sunderland, MA.

Kabsch, W., and C. Sander. 1983. Dictionary of protein secondary structure: pattern recognition of hydrogen-bonded and geometrical features. *Biopolymers.* 22:2577–2637.

Karshikoff, A., V. Spassov, S. W. Cowan, R. Ladenstein, and T. Schirmer. 1994. Electrostatic properties of two porin channels from *Escherichia coli*. *J. Mol. Biol.* 240:372–384.

Kerr, I. D., R. Sankararamakrishnan, O. S. Smart, and M. S. P. Sansom. 1994. Parallel helix bundles and ion channels: molecular modelling via simulated annealing and restrained molecular dynamics. *Biophys. J.* 67:1501–1515.

Kraulis, P. J. 1991. MOLSCRIPT: a program to produce both detailed and schematic plots of protein structures. *J. Appl. Crystallogr.* 24:946–950.

Lear, J. D., Z. R. Wasserman, and W. F. DeGrado. 1988. Synthetic amphiphilic peptide models for protein ion channels. *Science.* 240: 1177–1181.

Lim, C., D. Bashford, and M. Karplus. 1991. Absolute pKa calculations with continuum dielectric methods. *J. Phys. Chem.* 95:5610–5620.

Marrink, S. J., and H. J. C. Berendsen. 1994. Simulation of water transport through a lipid membrane. *J. Phys. Chem.* 98:4155–4168.

Marrink, S. J., O. Berger, D. P. Tieleman, and F. Jahnig. 1998. Adhesion forces of lipids in a phospholipid membrane studied by molecular dynamics simulations. *Biophys. J.* 74:931–943.

Mathew, M. K., and P. Balaram. 1983a. Alamethicin and related channel forming polypeptides. *Mol. Cell. Biochem.* 50:47–64.

Mathew, M. K., and P. Balaram. 1983b. A helix dipole model for alamethicin and related transmembrane channels. *FEBS Lett.* 157:1–5.

Mitton, P., and M. S. P. Sansom. 1996. Molecular dynamics simulations of ion channels formed by bundles of amphipathic α-helical peptides. *Eur. Biophys. J.* 25:139–150.

Molle, G., J. Y. Dugast, G. Spach, and H. Duclohier. 1996. Ion-channel stabilization of synthetic alamethicin analogs by rings of inter-helix H-bonds. *Biophys. J.* 70:1669–1675.

Roux, B. 1996. Valence selectivity of the gramicidin channel: a molecular dynamics free energy perturbation study. *Biophys. J.* 71:3177–3185.

Roux, B. 1997. Influence of the membrane potential on the free energy of an intrinsic protein. *Biophys. J.* 73:2980–2989.

Roux, B., and M. Karplus. 1991. Ion transport in a model gramicidin channel: structure and thermodynamics. *Biophys. J.* 59:961–981.

Roux, B., and M. Karplus. 1994. Molecular dynamics simulations of the gramicidin channel. *Annu. Rev. Biophys. Biomol. Struct.* 23:731–761.

Sankararamakrishnan, R., C. Adcock, and M. S. P. Sansom. 1996. The pore domain of the nicotinic acetylcholine receptor: molecular modelling and electrostatics. *Biophys. J.* 71:1659–1671.

Sansom, M. S. P. 1991. The biophysics of peptide models of ion channels. *Prog. Biophys. Mol. Biol.* 55:139–236.

Sansom, M. S. P. 1992. Proline residues in transmembrane helices of channel and transport proteins: a molecular modelling study. *Protein Eng.* 5:53–60.

Sansom, M. S. P. 1993. Structure and function of channel-forming peptaibols. *Q. Rev. Biophys.* 26:365–421.

Sansom, M. S. P. 1998. A first view of K^+ channels in atomic glory. *Curr. Biol.* 8:R450–R452.

Sansom, M. S. P., C. Adcock, and G. R. Smith. 1998a. Modelling and simulation of ion channels: applications to the nicotinic acetylcholine receptor. *J. Struct. Biol.* 121:246–262.

Sansom, M. S. P., L. R. Forrest, and R. Bull. 1998b. Viral ion channels: molecular modelling and simulation. *Bioessays.* 20:992–1000.

Sansom, M. S. P., I. D. Kerr, G. R. Smith, and H. S. Son. 1997a. The influenza A virus M2 channel: a molecular modelling and simulation study. *Virology.* 233:163–173.

Sansom, M. S. P., G. R. Smith, C. Adcock, and P. C. Biggin. 1997b. The dielectric properties of water within model transbilayer pores. *Biophys. J.* 73:2404–2415.

Sansom, M. S. P., D. P. Tieleman, and H. J. C. Berendsen. 1999. The mechanism of channel formation by alamethicin as viewed by molecular dynamics simulations. *Novartis Foundation Symp.* (in press).

Smart, O. S., J. Breed, G. R. Smith, and M. S. P. Sansom. 1997. A novel method for structure-based prediction of ion channel conductance properties. *Biophys. J.* 72:1109–1126.

Smart, O. S., J. M. Goodfellow, and B. A. Wallace. 1993. The pore dimensions of gramicidin A. *Biophys. J.* 65:2455–2460.

Smith, G. R., and M. S. P. Sansom. 1997. Molecular dynamics study of water and Na^+ ions in models of the pore region of the nicotinic acetylcholine receptor. *Biophys. J.* 73:1364–1381.

Smith, G. R., and M. S. P. Sansom. 1998. Dynamic properties of Na^+ ions in models of ion channels: a molecular dynamics study. *Biophys. J.* 75:2767–2782.

Tieleman, D. P., and H. J. C. Berendsen. 1996. Molecular dynamics simulations of a fully hydrated dipalmitoylphosphatidycholine bilayer with different macroscopic boundary conditions and parameters. *J. Chem. Phys.* 105:4871–4880.

Tieleman, D. P., and H. J. C. Berendsen. 1998. A molecular dynamics study of the pores formed by *E. coli* OmpF porin in a fully hydrated POPE bilayer. *Biophys. J.* 74:2786–2801.

Tieleman, D. P., J. Breed, H. J. C. Berendsen, and M. S. P. Sansom. 1998a. Alamethicin channels in a membrane: molecular dynamics simulations. *Faraday Disc.* (in press).

Tieleman, D. P., L. R. Forrest, H. J. C. Berendsen, and M. S. P. Sansom. 1998b. Lipid properties and the orientation of aromatic residues in OmpF, influenza M2 and alamethicin systems: molecular dynamics simulations. *Biochemistry.* 37:17554–17561.

Tieleman, D. P., S. J. Marrink, and H. J. C. Berendsen. 1997. A computer perspective of membranes: molecular dynamics studies of lipid bilayer systems. *Biochim. Biophys. Acta.* 1331:235–270.

Tieleman, D. P., M. S. P. Sansom, and H. J. C. Berendsen. 1999. Alamethicin helices in a bilayer and in solution: molecular dynamics simulations. *Biophys. J.* 76:40–49.

Tobias, D. J., K. C. Tu, and M. L. Klein. 1997. Atomic-scale molecular dynamics simulations of lipid membranes. *Curr. Opin. Colloid Interface Sci.* 2:15–26.

Unwin, N. 1995. Acetylcholine receptor channel imaged in the open state. *Nature.* 373:37–43.

Wallin, E., and G. von Heijne. 1998. Genome-wide analysis of integral membrane proteins from eubacterial, archean, and eukaryotic organisms. *Protein Sci.* 7:1029–1038.

Woolley, G. A., P. C. Biggin, A. Schultz, L. Lien, D. C. J. Jaikaran, J. Breed, K. Crowhurst, and M. S. P. Sansom. 1997. Intrinsic rectification of ion flux in alamethicin channels: studies with an alamethicin dimer. *Biophys. J.* 73:770–778.

Woolley, G. A., and B. A. Wallace. 1992. Model ion channels: gramicidin and alamethicin. *J. Membr. Biol.* 129:109–136.

You, S., S. Peng, L. Lien, J. Breed, M. S. P. Sansom, and G. A. Woolley. 1996. Engineering stabilized ion channels: covalent dimers of alamethicin. *Biochemistry.* 35:6225–6232.

Zhong, Q., Q. Jiang, P. B. Moore, D. M. Newns, and M. L. Klein. 1998a. Molecular dynamics simulation of an ion channel. *Biophys. J.* 74:3–10.

Zhong, Q., P. B. Moore, D. M. Newns, and M. L. Klein. 1998b. Molecular dynamics study of the LS3 voltage-gated ion channel. *FEBS Lett.* 427:267–270.